

# Simulation model for solar energy harnessing by the solar tunnel dryer

G. M. Kituu<sup>1</sup>, D. Shitanda<sup>1</sup>, C. L. Kanali<sup>1</sup>, J. T. Mailutha<sup>1</sup>,  
C. K. Njoroge<sup>2</sup>, J. K. Wainaina<sup>3</sup>, J. S Bongyereire<sup>4</sup>

(1. *Biomechanical and Environmental Engineering Department, Jomo Kenyatta University of Agriculture and Technology, Nairobi, Kenya;*

2. *Food Science and Technology Department, Jomo Kenyatta University of Agriculture and Technology, Nairobi, Kenya;*

3. *Institute of Computer Science and Information Technology, Jomo Kenyatta University of Agriculture and Technology, Nairobi, Kenya;*

4. *Africa 2000 Network (A2N)-Uganda)*

**Abstract:** Models were developed to predict global solar radiation and the energy harnessed by a solar tunnel dryer, and simulated in Visual Basic 6. In addition, the simulated data were compared with actual data. Using a 10% absolute residual error interval, the developed model achieved 78.4% and 83.3% performance for global solar radiation and energy harnessing, respectively. Further, the relationship between global solar radiation and the ten years mean satellite solar radiation, and that between the actual and simulated plenum chamber temperatures were linear, with coefficients of determination ( $R^2$ ) of 0.788 and 0.962. Thus, it shows that there is the existence of strong correlation between satellite and predicted global solar radiation, and between predicted and actual plenum chamber temperatures. Furthermore, Student's t-test did not show any significant difference between simulated and actual data for solar radiation and energy harnessing. Finally, this study shows that the developed model can be used to predict solar radiation and the energy harnessed by the solar tunnel dryer.

**Keywords:** modeling, tunnel-dryer, global, direct, solar-radiation, plenum-temperature

**Citation:** Kituu G. M., D. Shitanda, C. L. Kanali, J. T. Mailutha, C. K. Njoroge, J. K. Wainaina, and J. S Bongyereire. Simulation model for solar energy harnessing by the solar tunnel dryer. *Agric Eng Int: CIGR Journal*, 2010, 12(1): 91–98.

## 1 Introduction

In spite of abundant availability of solar energy in the tropics (Rabah, 2005), the determination of the quantity of energy available at any location has posed various challenges. This is because the quantity of solar energy available within these regions are dependent on the latitude, hour of the day, day of the year, altitude, and clearness of the sky (Al-Ajlan, Faris, and Khonkar., 2003; Jin, Yezheng, and Gang, 2005), and these values need to be determined and evaluated for the solar radiation incident at a location itself. In addition, the amount of global solar insolation at a place could be established by measurements, which is a tedious process, and many consumers of such information lack the tools to carry out

physical measurements. Besides, the common practice has been to develop models which can predict the energy incident at a particular location at any time. Such energy can then be used as an input variable in the design of solar energy application systems such as solar air and water heaters, and solar dryers among other uses. However, the exact science of the simulation and application of solar energy in the design of solar drying systems has not been adequately developed especially in sub-Saharan Africa, since most of the work in this field has been carried out in the developed world.

In the work reported by Garg and Prakash (2000) and Sukhatme (2003), several regional based models for evaluation of sunshine hours in which Africa is represented by Kisangani, in the Democratic Republic of Congo, Tamanrasset in Algeria and Malanje in Angola were developed. On the contrary, actual sunshine hours

are depended on localized weather, which is a function of geographical factors such as latitude, altitude, and cloud cover. In addition, the regions quoted above cannot represent the whole Africa in evaluation of sunshine hours.

Several authors have used different regional based models to predict the quantity of global solar energy available in specific regions of the world (Alfayo and Uiso 2002; Mechlouch and Brahim, 2008; El-Sebaai and Trabea 2005). In addition, the availability of solar energy is dependent on the location, and its weather patterns (Garg and Prakash, 2000; Sukhatme, 2003) and therefore no universal model can be used to determine the global solar energy available at any particular locality. The development of models, representing regions with similar geophysical conditions are thus necessary.

The design of the solar energy collection system is paramount in the efficient harnessing of solar energy by a solar drying system. The cover, the collector plate and the moving air have been identified (Plantier, Fraisse and Achard, 2007) as the most important parts of solar energy harnessing design. These parts relate to transmission of solar energy into the collector and any reflective as well as the radiative losses from the collector through the cover plate, and the absorption and harnessing of energy from the collector plate to the drying air. Models of global solar energy reception and harnessing of the energy incident on a solar tunnel dryer for regions in Kenya are lacking. Therefore, this study was conducted to develop a computer model to simulate: 1) the global solar radiation incident at Juja, Kenya, and 2) the harnessing of solar energy by the tunnel section of a solar tunnel dryer.

## 2 Materials and methods

### 2.1 Description of the experimental site

The experimental site was located at the Biomechanical and Environmental Engineering Department of the Jomo Kenyatta University of Agriculture and Technology, in Juja township, 10 km West of Thika town and 45 km East of Nairobi, Kenya. The latitude, longitude and altitude of the location are

1.18°S, 37°E and 1,460 m above sea level, respectively. The region experiences cold, rainy seasons between April and August, in October and December each year, the rest of the period being dry hot seasons (Watako et al., 2001). The ten year mean clearness index for Juja in the cold rainy season is 0.47, while during the dry hot seasons its 0.66 (NASA).

### 2.2 Global solar radiation model

Using models developed by Jin, Yezheng, and Gang. (2005), and El-Sebaai and Trabea (2005) the values of  $I_b$  (direct solar radiation) and  $I_d$  (diffuse solar radiation) are computed from the total solar radiation. The extra-terrestrial solar energy incident radiation on a horizontal surface  $H_0$  is given by Equation (1) (Al-Ajlan, Faris, and Khonkar, 2003), where  $n$  is the day of the year,  $\varphi$  is the latitude (degrees),  $\delta$  is the angle of declination (degrees) and  $\omega_s$  is the sunset or sunrise hour angle (degrees).

$$H_0 = \frac{24(1367)}{\pi} \left( 1 + 0.033 \cos \left( \frac{360n}{365} \right) \right) (\cos \varphi \cos \delta \sin \omega_s + \omega_s \sin \varphi \sin \delta) \quad (1)$$

The declination, and sunset (or sunrise) hour angle in Equation (1) are determined from the expression in Equations (2) and (3), respectively (Garg and Prakash, 2000)

$$\delta = 23.45 \sin \left( 360 \left( \frac{284 + n}{365} \right) \right) \quad (2)$$

$$\omega_s = \pm \cos^{-1} (-\tan \varphi \tan \delta) \quad (3)$$

Several authors have developed different region and location based models for the prediction of global solar radiation on a horizontal surface, among them Al-Ajlan, Faris, and Khonkar (2003), Jin, Yezheng, and Gang (2005), Tarhan and Sari (2005). Solar radiation at any location is a function of several parameters, including latitude, declination, hour angle and altitude (Jin, Yezheng, and Gang, 2005). The model developed by (Jin, Yezheng, and Gang, 2005) is of the form given in Equation (4), where  $H'_g$  is the general daily global solar radiation on a horizontal surface ( $\text{MJ}/\text{m}^2$ ),  $S_p$  is the number of possible sunshine hours in a particular day,  $S_a$  the number of actual sunshine hours in a particular day, and  $H_{asl}$  the height (km) above sea level.

$$H'_g = H_0 \left\{ \begin{array}{l} (0.0218 + 0.0033\varphi + 0.0443H_{ast}) + (0.9979 - \\ 0.0092\varphi - 0.0852H_{ast}) \frac{S_p}{S_a} + (-0.5579 + \\ 0.012\varphi - 0.1005H_{ast}) \left( \frac{S_p}{S_a} \right)^2 \end{array} \right\} \quad (4)$$

A set of equations to determine the hourly global solar radiation  $I_g$  (W/m<sup>2</sup>) incident on a horizontal surface at Juja, Kenya, were developed as in Equation (5)-(7), in which  $\omega$  is the hour angle (degrees) such that for  $n \leq 120$ ,

$$I_g = 1.2545 * \left( \frac{\pi}{24} H'_g (a_j + b_j \cos \omega) \right) \left( \frac{(\cos \omega - \cos \omega_s)}{\left( \sin \omega_s - \frac{\pi \omega_s}{180} \cos \omega_s \right)} \right) \left( 1 + 0.033 \cos \left( \frac{360n}{365} \right) \right)^4 \cos^2 \delta \quad (5)$$

while for  $120 < n < 310$

$$I_g = 1.0816 * \left( \frac{\pi}{24} H'_g (a_j + b_j \cos \omega) \right) \left( \frac{(\cos \omega - \cos \omega_s)}{\left( \sin \omega_s - \frac{\pi \omega_s}{180} \cos \omega_s \right)} \right) \left( 1 + 0.033 \cos \left( \frac{360n}{365} \right) \right) \cos^2 \delta \quad (6)$$

and for  $310 \leq n \leq 365$

$$I_g = 1.4235 \left( \frac{\pi}{24} H'_g (a_j + b_j \cos \omega) \right) \left( \frac{(\cos \omega - \cos \omega_s)}{\left( \sin \omega_s - \frac{\pi \omega_s}{180} \cos \omega_s \right)} \right) \left( 1 + 0.033 \cos \left( \frac{360n}{365} \right) \right)^2 \cos^4 \delta \quad (7)$$

The parameters  $a_j$  and  $b_j$  are evaluated using the expressions in Equation (8)-(9) (Al-Ajlan et al., 2003)

$$a_j = 0.409 + 0.5061 \sin(\omega_s - 60) \quad (8)$$

$$b_j = 0.6609 - 0.4767 \sin(\omega_s - 60) \quad (9)$$

### 2.3 Energy harnessing model

The solar tunnel dryer system used in this study (Figure 1) was developed at the Biomechanical and Environmental Engineering department, Jomo Kenyatta University of Agriculture and Technology. It consists of

two main components: the tunnel and the chimney chambers. The tunnel is used for heating the drying air before it enters the chimney. The tunnel section measures 2.4 m long, 1.2 m wide and 0.54 m high. It has a rectangular mild-steel collector plate, painted black for enhanced absorption and emission of solar energy, and an acrylic cover located above the collector plate. The acrylic cover acts as a green-house to absorbed solar-energy which results in increased energy concentration in the chamber. The bottom side of the tunnel section is covered with aluminium painted galvanised iron (GI) sheet to reflect energy incident on the surface. Similarly, the rear side wall of the tunnel chamber is made of aluminium coated GI sheet. The front wall of the chamber has two sets of overlapping doors, to facilitate instrumentation of the tunnel chamber, for data collection. The inner walls of the doors are lined with aluminium coated GI sheets. The bottom and the side walls of the sheets are insulated with polystyrene sheets sandwiched between the inner and outer GI sheets to minimise energy losses.



Figure 1 Solar tunnel dryer

The chimney drying chamber measures 1.2 m by 0.9 m by 0.7 m for the rectangular cross-section, and 1.2 m × 0.7 m at the bottom and 0.2 m by 0.2 m at the narrow end. It is made of GI sheets, with the inner walls coated with aluminum while the outer walls are painted black. An exhaust system secured above the chimney drying chamber is lined with acrylic to enable solar heating of the exhaust air, to enhance forced convection.

Analysis of the energy collection in the tunnel section is based on the assumptions; that there is no heat gain to or loss from the solar energy collector, except heat losses which could be evaluated using the overall heat loss coefficient; that the energy harnessed is evaluated under steady state conditions, and that the dryer walls and any trays in the tunnel section are adiabatic. Besides, the energy harnessed by a solar air heater manifests in the rising of the temperatures of the drying air. The energy analysis by Garg and Prakash (2000) and Sukhatme (2003) gives the temperature profile along the tunnel section of the dryer. Based on this analysis, and assuming the inlet air temperature to be equal to the ambient air temperature, the plenum chamber temperature  $T_p$  was developed as in Equation (10), where  $T_i$  is the inlet air temperature,  $I_c$  is the solar radiation absorbed by a collector plate per unit area per unit time ( $\text{W/m}^2$ ),  $U_L$  is the total energy loss coefficient of the solar collector ( $\text{W/m}^2\text{-K}$ ),  $A_c$  is the collector plate surface area ( $\text{m}^2$ ),  $F'$  is the collector efficiency factor (dimensionless),  $\dot{m}_a$  is the air flow rate ( $\text{kg/s}$ ),  $C_{pa}$  is the specific heat of air ( $\text{J/kg-K}$ ),  $H$  is the humidity of air in the tunnel section ( $\text{kg/kg}$ ), and  $C_{pv}$  the specific heat of water vapour ( $\text{J/kg-K}$ ).

$$T_p = T_i + \frac{I_c}{U_L} \left( 1 - \exp \left( - \frac{A_c F' U_L}{\dot{m}_a (C_{pa} + H C_{pv})} \right) \right) \quad (10)$$

A solar beam incident on a collector surface undergoes reflection, refractive transmission and absorption (Sukhatme, 2003), and the energy absorbed per unit area of the collector plate per unit time  $I_c$ , is given by Equation (11) (Garg and Prakash, 2000; Al-Ajlan et al., 2003), where  $I_b$  is the direct solar radiation incident on a horizontal surface ( $\text{W/m}^2$ ),  $R_b$  is conversion factor for the direct solar radiation,  $I_d$  is the diffuse solar radiation incident on the horizontal surface ( $\text{W/m}^2$ ),  $R_d$  is the diffuse radiation conversion factor,  $R_r$  is the global radiation conversion factor,  $A_b$  is the albedo of the ground and  $(\tau\alpha)_e$  is the transmissivity-absorptivity product.

$$I_c = (I_b R_b + I_d R_d + (I_b + I_d) R_r A_b) \times (\tau\alpha)_e \quad (11)$$

The daily global solar radiation for Juja, Kenya,

$H_g$  ( $\text{MJ/m}^2$ ), was obtained by summing up the hourly global solar radiation for Juja,  $I_g$  in Equation (5)-(7), from sunrise to sunset as in Equation (12), where  $S_s$  is the sunset hour and  $S_r$  is the sunrise hour.

$$H_g = \sum_{S_r}^{S_s} I_g \quad (12)$$

The daily diffuse radiation, ( $H_d$ ,  $\text{MJ/m}^2$ ) depends on the hour angle, and the cloudiness ratio  $k_t$  given by Equation (13) (Al-Ajlan, Faris, and Khonkar, 2003; Tarhan and Sari, 2005)

$$k_t = \frac{H_g}{H_0} \quad (13)$$

The daily diffuse radiation is evaluated from the expressions (14)-(15), given by (Garg and Prakash., 2005) as follows:

For  $\omega_s > 81.4^\circ$  and  $k_t \leq 0.8$

$$H_d = H_g (1.311 - 3.022k_t + 3.427k_t^2 - 1.821k_t^3) \quad (14)$$

For  $\omega_s \leq 81.4^\circ$  and  $0.3 \leq k_t < 0.8$

$$H_d = H_g (1.311 - 3.560k_t + 4.189k_t^2 - 2.137k_t^3) \quad (15)$$

Besides, the hourly diffuse solar radiation,  $I_d$  ( $\text{W/m}^2$ ) based on Equation (14) and (15) is expressed as in Equation (16) (Al-Ajlan, Faris, and Khonkar, 2003)

$$I_d = \left( \frac{\pi}{24} H_d \right) \left( \frac{\cos \omega - \cos \omega_s}{\left( \sin \omega_s - \frac{\pi \omega_s}{180} \cos \omega_s \right)} \right) \quad (16)$$

The hourly direct solar radiation incident  $I_b$  ( $\text{W/m}^2$ ) on a horizontal surface was computed using Equation (17) (Garga and Prakash, 2000)

$$I_b = I_g - I_d \quad (17)$$

Based on Equation (16), (17); Equation (11) could be evaluated, which led to the determination of  $I_c$ , and eventually the plenum chamber temperature in Equation (10).

## 2.4 Data acquisition and model performance

### 2.4.1 Simulation algorithm

A visual basic algorithm was developed to simulate the global solar radiation on a horizontal surface (Equation (5)-(7)), and the solar energy harnessing in the tunnel section of the dryer (Equation (11)). The environmental input parameters included sunshine hours,

relative humidity, ambient air temperature and velocity of the drying air. Sunshine hours were obtained from field station weather records at the Biomechanical and Environmental Department of the Jomo Kenyatta University of Agriculture and Technology. The algorithm developed was able to simulate hourly global solar radiation values, and subsequently the solar dryer energy harnessing in-terms of plenum chamber temperatures. A flow chart for the simulation process was as shown in Figure 2.

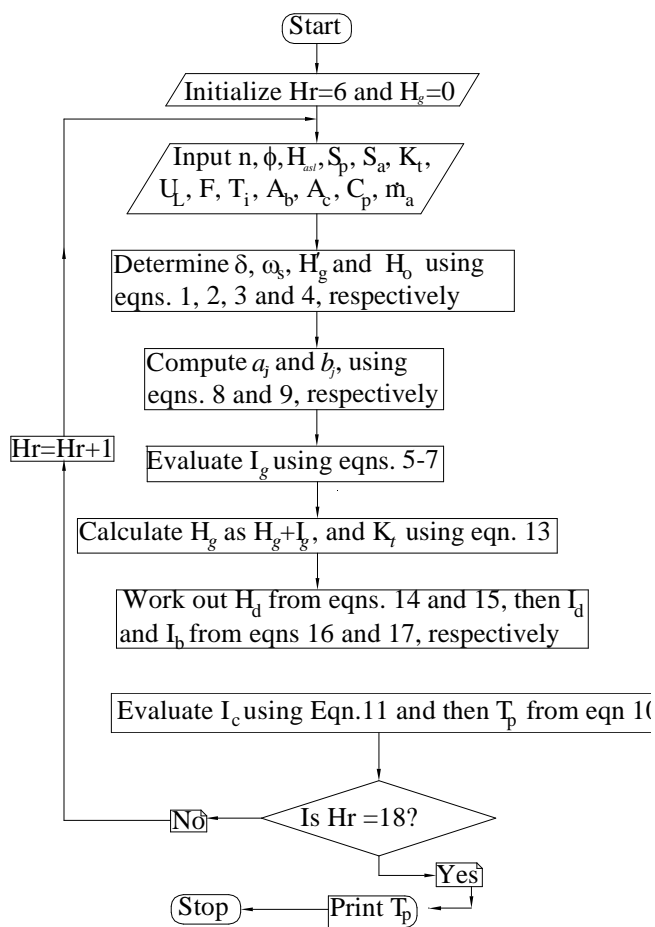


Figure 2 Flow chart for the simulation algorithm

2.4.2 Experimental set-up

Figure 3 presents a schematic diagram of the experimental set up. The setup was used to measure the tunnel chamber temperatures, in order to evaluate the energy harnessing model. Inlet air and plenum chamber temperatures were measured at points A and B, respectively, using thermocouples, which logged the temperatures to an automatic electronic data logger (Thermodac Eto Denki E, Shimadzu, Japan).

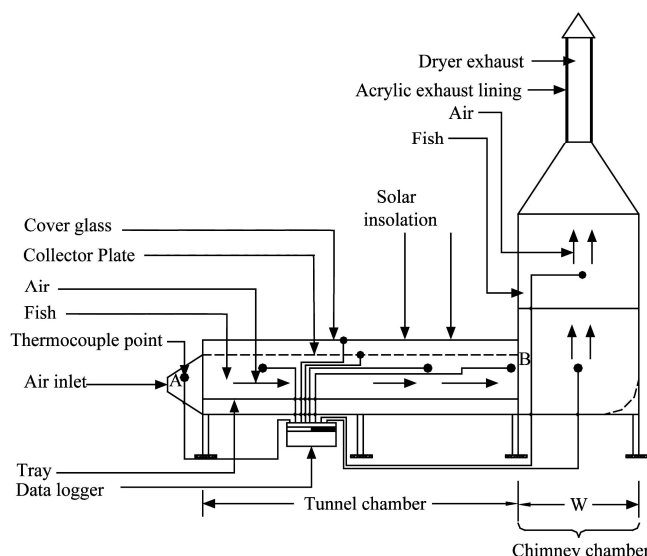


Figure 3 Schematic representation of the solar tunnel dryer

2.4.3 Simulation model performance

Daily ten years (viz: 1996-2005, inclusive) global solar radiation data was downloaded from NASA weather data station. The simulated daily global solar radiation data was compared with the mean of ten years satellite global solar radiation data. In addition, the percent absolute residual errors, between simulated and ten years mean satellite solar radiation data points were determined from Equation (18) (Uluko et al., 2007), where  $E_r$  is percent residual error,  $X_{sim}$  is the simulated value, and  $X_{act}$  is actual value.

$$E_r = \left( \left| \frac{X_{sim} - X_{act}}{X_{act}} \right| \right) \times 100 \quad (18)$$

The prediction performance of the model  $\eta_m$ , at  $m\%$  residual error interval was evaluated using Equation (19), in which  $N_m$  and  $N_t$  represent the number of observations within the interval, and the total trial observations, respectively.

$$\eta_m = \left( \frac{N_m}{N_t} \right) \times 100 \quad (19)$$

Linear regression analysis was also carried out in MS Excel 2007 to relate the predicted and the simulated global solar radiation. In addition, Student's  $t$ -test was used to test for significant difference between the simulated and actual data. Similarly, the performance of the energy harnessing model was determined from residual error and regression analysis, and Student's  $t$ -test.

### 3 Results and discussion

#### 3.1 Solar energy reception model

The daily annual simulated and 10-year mean (1996-2005) satellite global solar radiation are presented in Figure 4. The figure shows fluctuations with global maxima and minima in February and July, and local maxima and minima in October and November, respectively. The maxima and minima coincide with the hottest and cold seasons in the region as reported earlier.

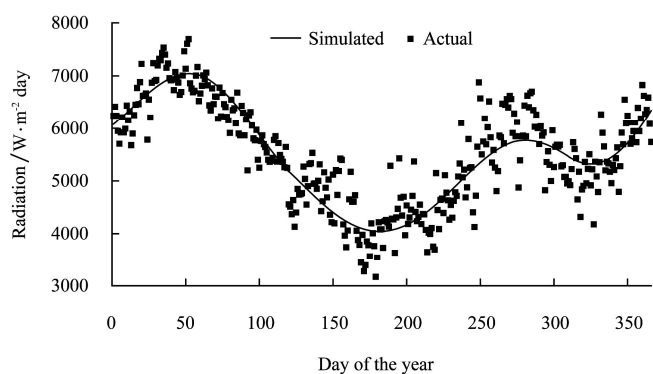


Figure 4 Annual variation of global solar radiation (both simulated and ten year mean)

The absolute percentage residual error between the simulated and the mean of ten year satellite solar radiation ranged from 0.04%-27.70%. The performance of the global solar radiation model at 10% residual error was evaluated as 78.4%. Using regression analysis, a linear relation between the simulated and actual solar radiation was established, with a regression equation of the form shown in Equation (20), where  $H_{sim}$  is simulated solar radiation, and  $H_{act}$  is actual solar radiation.

$$H_{sim} = 0.8215H_{act} + 970.90 \quad (20)$$

$$R^2 = 0.788.$$

This behaviour is consistent with observations by Mechlouch and Brahim (2008). Since the coefficient of determination in Equation (20) is high, there exists a strong correlation between the simulated radiation and the mean satellite solar radiation. Using analysis of variance, there was no statistical difference between simulated and actual global solar radiation, at 5% level of significance ( $t_{stat} = 0.17$ ,  $t_{crit} = 1.65$ ). Therefore the developed model can be used to simulate global solar radiation incident on a horizontal surface.

Regression analysis revealed a linear relation in the variation in both the solar radiation incident on and that absorbed by the collector plate, with the global solar radiation. The values of  $R^2$  for the change of the solar radiation incident on, and that absorbed by a collector plate with the global solar radiation were high (0.9703 and 0.9756, respectively), indicating the existence of a strong correlation between both the solar radiation incident on, and that absorbed by a collector plate and the global solar radiation.

#### 3.2 Solar energy harnessing by the tunnel section of solar tunnel dryer

The mean of five days inlet, experimental and simulated plenum chamber temperature are shown in Figure 5. The harnessing of solar energy and its conversion to heat energy was demonstrated by the relatively high plenum chamber temperatures compared to the inlet air temperatures. In addition, the predicted plenum chamber temperatures were higher than the experimental plenum chamber temperatures, and this could be attributed to non-useful energy dissipation from the tunnel chamber. For instance, between 7 to 10 am, energy was used to vaporize moisture which had condensed on the collector plate surface, and this must have resulted in reduced actual plenum chamber temperatures in the morning. Besides, minimal unnoticeable energy losses might have been taken place as a result of poor air tightness of the chamber resulting in energy losses, and hence the lower experimental chamber temperature compared to the simulated plenum chamber temperatures.

The plenum chamber temperature increased from low values in the morning and attained maximum values between noon and 13 hours, before reducing to a minimum, for the sets of temperatures under analysis. The peak temperatures corresponded to the maximum value of global solar radiation are aligned with observations by Kaplanis (2006), Trabea (2000) and Pidwimy (2006). Additionally, plenum chamber temperatures were higher at the end of the day, than at the start of the day, which could be attributed to the continued re-radiation of absorbed heat from the ground.

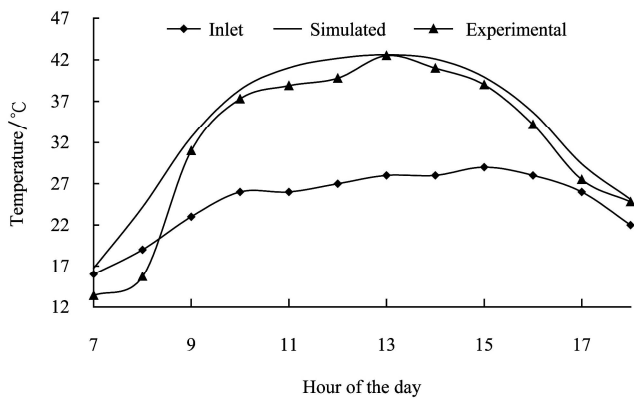


Figure 5 Daily experimental and simulated plenum and inlet air temperatures

The absolute residual error between the simulated and the experimental plenum chamber temperatures ranged between 0.28% and 53.89%. The higher percent residual error was prevalent in the morning hours, when energy was expended in evaporating condensate on the collector surface. The performance of the plenum chamber temperature model at 10% residual error interval was 83.3%. The relation between the experimental and plenum chamber temperature was established, through regression analysis to be linear, with a high value of  $R^2$  (0.9621). Thus, a strong correlation exists between the simulated and experimental plenum chamber temperatures. Furthermore, based on Student's  $t$ -test, there was no statistical difference between the simulated and plenum chamber temperatures at 5% level of significance ( $t_{stat}=0.55$ ,  $t_{crit}=1.72$ ). Therefore the model developed can be used to predict the harnessing of solar energy by the solar tunnel dryer.

#### 4 Conclusions

Models to predict global solar radiation, and the energy harnessing by a solar tunnel dryer were developed. A Visual Basic 6 computer based algorithm was

developed to simulate the global solar radiation on a horizontal ground, and the energy harnessing by the tunnel dryer. The model performance at 10% residual error interval was 78.4% and 83.3%, respectively, for global solar radiation and plenum chamber temperature. Linear relations existed between the simulated and mean of satellite global solar radiation, and simulated and actual plenum chamber temperature. The correlation between the simulated and satellite solar radiation was strong since the coefficient of determination was high ( $R^2=0.788$ ). Similarly, a strong correlation existed between the simulated and actual plenum chamber temperature ( $R^2=0.9621$ ). The relation between solar radiation absorbed by collector plate and global solar radiation was linear, with a high value of  $R^2$  (0.9756) indicating a strong relation between the solar radiation absorbed by a collector plate and the global solar radiation. In addition, based on Student's  $t$ -test, there was no significant difference between simulated and actual data for both solar radiation and energy harnessing. The above results show that the developed models can be used to predict global solar radiation at Juja, Kenya, and energy harnessed by solar tunnel dryer. These results are useful in the control of the drying process of agricultural produce as the drying conditions can be predicted.

#### Acknowledgements

The authors wish to acknowledge the financial support extended to this research by VicRes, a SAREC sponsored Lake Victoria Research Program. In addition, the support in terms of research facilities from the Jomo Kenyatta University of Agriculture and Technology is acknowledged.

#### References

- Al-Ajlan S. A., H. Al Faris, and H. Khonkar. 2003. A simulation modeling for optimization of flat plate collector design in Riyadh, Saudi 'Arabia'. *Renewable Energy*, 28(No.): 1325–1339.
- Alfayo R., and C. B. S. Uiso. 2002. Global solar radiation distribution and available solar energy potential in Tanzania. *Physica Scripta*. T97, 91–98.
- De Souza J. L., R. M., a Nicácio, and M. A. L Moura. 2005. Global solar radiation measurements in Maceio, Brazil. *Renewable Energy*, 30(3): 1203–1220.

- El-Adawi M. K. 2002. New approach to modeling a flat plate collector: The Fourier transform technique. *Renewable Energy*, 26, 489–506.
- El-Sebaei A. A., and A. A. Trabea. 2005. Estimation of global solar radiation on horizontal surfaces over Egypt. *Egypt J. Solids*, 28(1): 163–175.
- Ezekoye B. A., and O. M. Enebe. 2006. Development and performance evaluation of modified integrated passive solar grain dryer. *The Pacific Journal of Science and Technology*, 7(2): 185–190.
- Garg H. P., and J. Prakash. 2000. *Solar energy: Fundamentals and applications*, 1st Revised ed. Tata McGraw Hill Publishers, New Delhi, India.
- Jin Z. W. Yezheng, and Y. Gang. 2005. General formula for estimation of monthly average daily global solar radiation in China. *Energy and Conservation Management*, 46(2): 257–268.
- Kaplanis S. N. 2006. New methodologies to estimate the hourly global solar radiation; Comparisons with existing models. *Renewable Energy*, 31(6): 781–790.
- Mechlouch R. F., and A. B. Brahim. 2008. A global solar radiation model for the design of solar energy systems. *Asian Journal of Scientific Research*, 1(3): 231–238.
- Pidwimy M. 2006. *Daily and annual cycles of temperature. fundamentals of physical geography*, 2nd ed; British Columbia, Canada.
- Plantier C., G. Fraisse, and G. Achard. 2007. Development and experimental validation of a detailed Flat-Plate solar collector model. in the *Proceedings of the International Agricultural Engineering Conference-2007*, Asian Institute of Technology, Bangkok.
- Rabah K .V. O. 2005. Integrated solar energy systems for rural electrification in Kenya. *Renewable Energy*, 30(1): 23–42.
- Sukhatme P.K. 2003. *Solar energy: Principles of thermal collection and storage*. 2nd ed, Tata McGraw-Hill Publishing, New Delhi.
- Tarhan S., and A. Sari. 2005. Model selection for global and diffuse radiation over the Central Black Sea (CBS) Region of Turkey. *Energy Conservation and Management*, 46(4): 605–613.
- Trabea A. A. 2000. Analysis of solar radiation measurements at Al-Arish area, North Sinai, Egypt. *Renewable Energy*, 20(1): 109–125.
- Uluko H., Mailutha J. T., Kanali C. L., and D. Shitanda. 2007. A finite element prediction of temperature distribution in a solar grain dryer. *The Kenya Journal Of Mechanical Engineering; KJME*, 3(1): 45–53.
- Watako A. O., C. K. Ndung'u, K. Ngamau, and H. Suguira. 2001. The effect of rootstock on budtake and budgrowth vigour of rose(*Rosa Spp*) cultivar (First Red). *Journal of Agriculture, Science and Technology*, 1(2): 57–67.